PREEQUILIBRIUM NEUTRON EMISSION IN (p, xn) REACTIONS WITH 80-160 MeV PROJECTILES*

W. Scobel and M. Trabandt
University of Hamburg, West Germany

H.M. Blann, B.A. Pohl, and B.R. Remington
Lawrence Livermore National Laboratory, California 94550

R. Bonotti
Istituto di Risica Generale Applicate dell' Universita Milano, Italy

S.M. Grimes
Ohio University, Athens, Ohio 45701

R.C. Byrd and C.C. Foster
Indiana University Cyclotron Facility, Bloomington, Indiana 47405

The reactions $^{90}Zr,^{208}Pb(p,xn)$ have been studied in the neutron continuum $E_n \geq 20$ MeV and the angular range $0° \leq \theta \leq 145°$ for projectile energies of 80, 120, and 160 MeV. Results are compared to predictions of phenomenological parameterizations, a semiclassical precompound and a quantum statistical multistep model.

Spectral and angular distributions of continuum neutrons from (p,n) reactions are particularly appropriate to study the preequilibrium reaction phase, because a competing break up mechanism in the case of complex projectiles as well as inelastic projectile scattering that would complicate the interpretation of the data are excluded. In the last ten years the (p,n) equilibration process has been studied quite frequently[1] with projectile energies up to 45 MeV.

Several nuclear models consider the equilibration to proceed through increasingly complex configurations of single particle excitations. On one hand there is the class of semiclassical models that apply the quasifree intranuclear nucleon-nucleon collision picture; they yield convincing results for angle integrated nucleon energy spectra,[2] but mostly fail to reproduce double differential cross sections in the backward hemisphere.[3,4] For the latter, finite size effects, incorrect treatment of higher chance nucleon emission and of the balance between single and multiple nucleon emission have been blamed.[2,5]

Quantum statistical models have been presented[6,7] that succeeded in describing also (p,n) and (p,p') data for $\theta > 90°$. The Statistical Multistep Model[7] provides excellent agreement not only in the energy regime of prevailing Multistep Compound (SMCE)[8] or Direct (SMDE)[9] emission, but also in the transition region.[1] The residual interaction strength V_0 in this model has been brought to consistency[10] with direct reaction results. The phenomenological model of Kalbach and Mann[11] finally may be considered a derivative of the exciton and the Statistical Multistep Model.

The contribution of preequilibrium emission to the nucleon yield increases with projectile energy. Therefore, accurate (p,n) data for $E_p > 50$ MeV that extend with good energy resolution and low background to very backward angles would provide a crucial test of

both semiclassical and quantal preequilibrium models. This data, however, is scarcely[11] available.

In this report we present first results from a study of the (p,n) continuum for $E_p = 80.5$, 120 and 160 MeV in the angular range $0° - 145°$ for the targets ^{90}Zr and ^{208}Pb. The results will be compared on an absolute scale to a semiclassical[12] as well as a quantum statistical[7] model and with the recent parameterization of Kalbach.[13]

The time-of-flight (TOF) experiment has been performed at the IUCF. A burst separation of 1.8 μs was achieved with the stripper loop.[14] The long beam-off time allowed neutron time-of-flight spectroscopy with high resolution over a broad dynamic range. The magnetic beam swinger[15] was operated with deflection angles of 0°, 11°, and 24°, respectively, to cover the angular range from 0° to 144° with 5 fixed detectors; the TOF path lengths varied from 11 m for the most backward to 61 m for the most forward detector. The neutron detectors consisted of cylindrical cells (30.5 cm diam. $\times$ 20.3 cm) filled with the liquid scintillator BI501. Sheets of plastic scintillator were placed in front and on top of the detectors to discriminate against protons and to suppress cosmic radiation. It was necessary to perform n-γ pulse shape discrimination; Fig. 1 shows the excellent discrimination features of this large detector. Background was measured by placing tubes of appropriate diameter filled with water as shadow bars midway between target and detectors; their lengths corresponded to flux attenuations of at least 97% for $E_n \leq 160$ MeV. Conversion of the TOF results (cf. Fig. 2) into energy spectra was performed with the efficiencies from Ref. 16.

The energy spectra shown in Fig. 3 represents a selection from $^{90}Zr(p,n)$ at $E_p = 120$ and 160 MeV including two independent measurements at $\theta = 24°$. The giant and analog resonance structure visible (in full resolution) at 0° is in quantitative agreement with recent results.[17] The spectra undergo a characteristic transition from a flat energy dependence in the forward continuum to an exponential shape at backward angles; their slopes, however, exceed the ones expected for equilibrated systems by more than a factor of 3 (Table I). Also, there is no indication at low energies E_n for an increase of the cross section with θ.

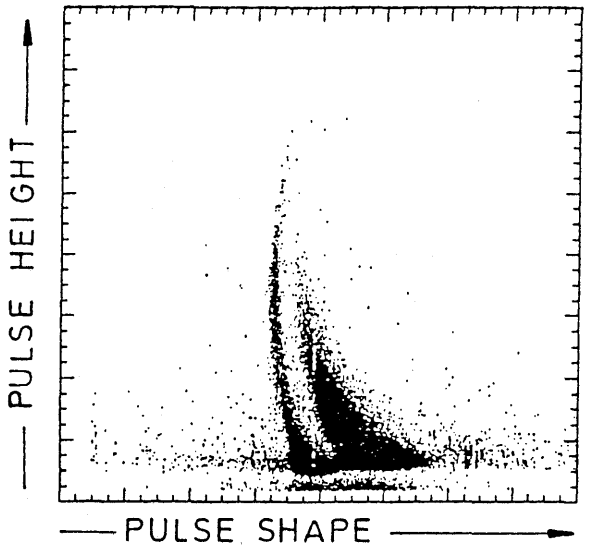

Figure 1. Scatter plot of pulse height vs. pulse shape signal ($E_p = 80$ MeV).

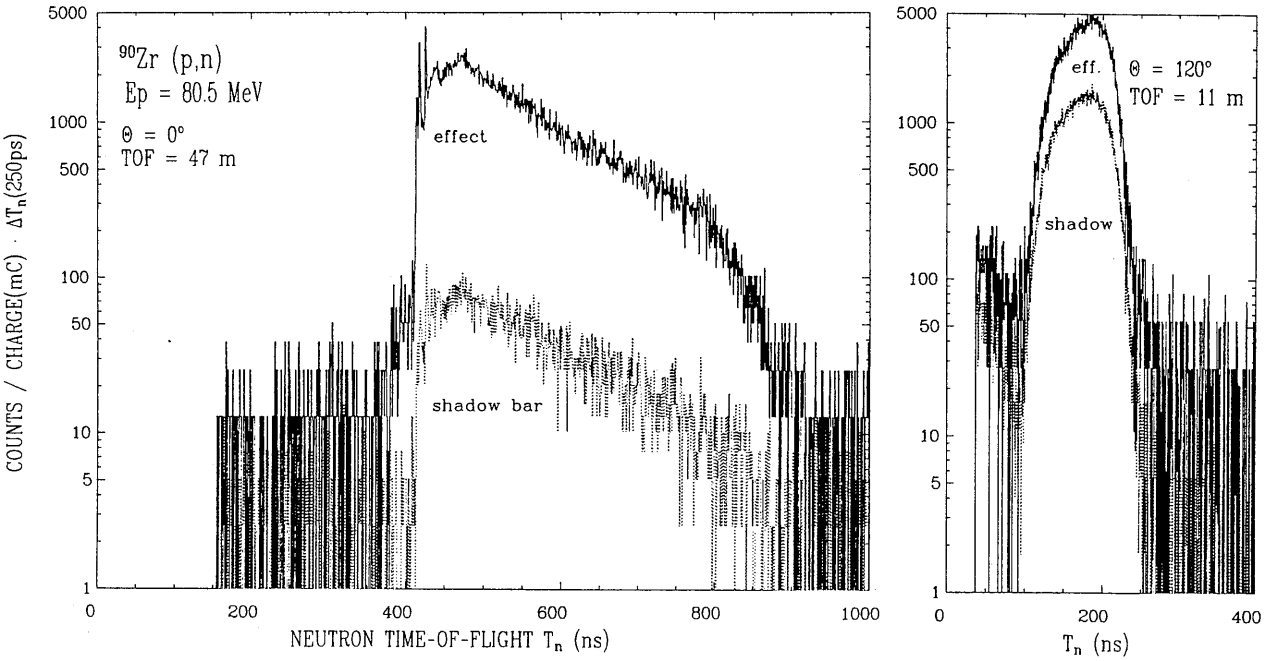

Figure 2. TOF spectra of effect and shadow bar run.

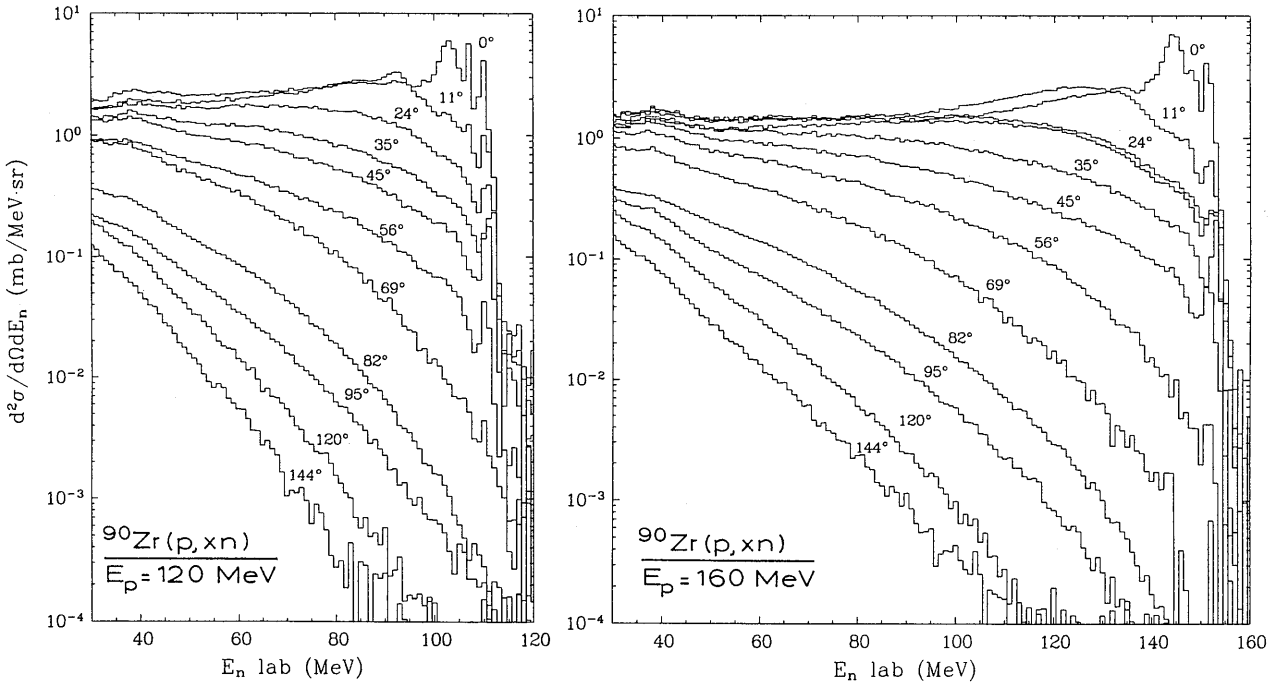

Figure 3. Energy spectra for a selection of angles in 1 MeV bins. The g.s. Q-value is −6.9 MeV.

Table I: Excitation energies and temperatures of ^{90}Zr + p and the slopes T(θ) of the most backward neutron spectra (in MeV).

E_p	80.5	120	160
E^*_{CN}	87.2	126.3	165.8
T_{CN}	2.8	3.3	3.8
T(θ=144°)	7.2	9.0	11.4

The dominant reaction mechanism therefore seems to be the SMDE type with only small SMCE contributions. If so, the data should agree with the systematics condensed into a parameterization of double differential cross sections in the spectral continuum[13]:

$$\frac{d^2\sigma}{d\Omega d\epsilon} = a_0^{MSD} \exp(a\cos\theta) + a_0^{MSC} \exp(a\cos\theta) + \exp(-a\cos\theta) \qquad (1)$$

Here, a_0^{MSD} and a_0^{MSD} fix the absolute cross sections of the multistep direct and compound emission, respectively, and have to be taken from a reaction model. The slope parameter a(E_p,ϵ) depends not only on the energy ϵ of the ejectile but also on the type and the energy E_p of the projectile. Its parameterization has been derived[13] from a broad range of angular distributions for light ($A \leq 4$) projectiles and ejectiles with energies up to 600 MeV. Here, Eq. (1) will be applied under the assumption of 100% MSD contribution.

Fig. 4 demonstrates that our data exhibit a dependence of the shapes on E_p. Therefore they rule out the preceding[18] parameterization intended for lower ($E_p < 80$ MeV, $\epsilon \leq 45$ MeV) energies, whereas Eq. (1) works well. For higher projectile energies E_p and a given neutron energy the angular distributions turn flatter and thus may indicate the importance of higher order steps with increasing inelasticity.

The dependence of the angular distributions on E_n is very pronounced. For $E_p = 160$ MeV we observe (cf. Fig. 5) at $E_n = 40$ MeV a reduction of the cross sections from very forward to backward angles by a factor 10, whereas at $E_n = 140$ MeV the distribution covers already 5 orders of magnitude in the region experimentally accessible. The normalized results of Eq. (1) follow this shape transition reasonably well which is another indication for the dominance of the MSD mechanism. Also shown in Fig. 5 is the prediction of a semiclassical model – in this case the geometry dependent hybrid model (GDH) with the assumption of a pure intranuclear nucleon-nucleon scattering mechanism. It reproduces the angle integrated spectrum on an absolute scale within a factor of no more than 2, but underestimates the yield at higher angles even more than observed[19] for lower proton energies. In contrast, the discrepancies at low angles are not of a principal nature.[3]

The multistep model of Feshbach et al.[7] treats the nuclear reaction as a sequential process chaining stages with increasing complexity. At each stage n it differs between two

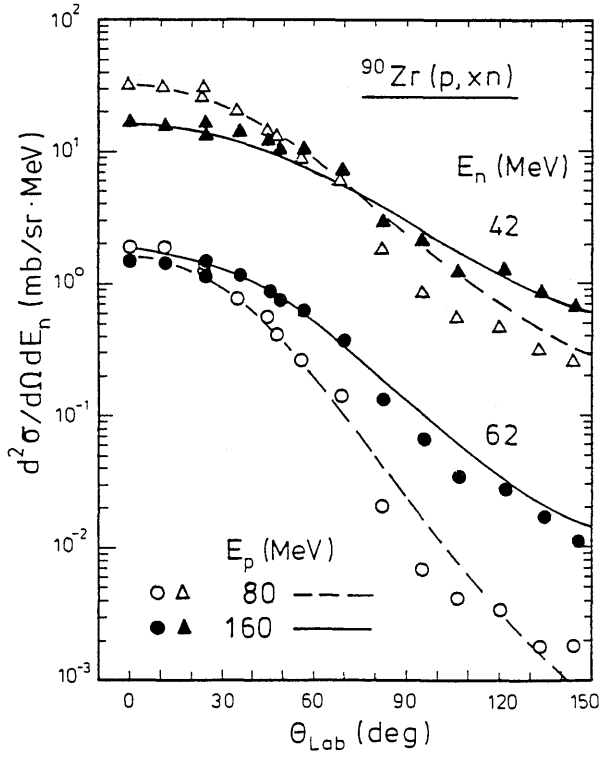

Figure 4. Angular distribution of 42 MeV and 62 MeV neutrons for different projectile energies. Curves are the normalized results of Eq. (1).

classes of states or reaction amplitudes. The SMDE mechanism proceeds only through states with at least one nucleon being unbound, whereas SMCE proceeds only through particle bound states. The calculation of the cross section as an incoherent sum of both contributions has been developed by Bonetti et al.[8-10] by using a Yukawa type potential with range $r_0 = 1$ fm and depth $V_0 = 26 \pm 1$ MeV as residual interaction causing the $n-1 \rightarrow n$ transitions. A recent application to (p,n) data for $E_p = 25$ MeV may be found elsewhere.[1]

So far we have applied this model to the 80.5 MeV data only. We have used the optical model potential of Schwandt et al.[20] for protons and a straight forward modification of it for neutrons. The results are given in Fig. 6. The shape of the angular distributions is well reproduced in all cases. The calculations demonstrate the importance of the higher order steps even for the highest neutron energies. The experimental data is, however, incompatible with calculations applying $V_0 = 25$ MeV. A reduction of V_0 to 20 MeV eliminates this deficiency. It seems improbable that this renormalization reflects an incorrect application of partial state densities that were derived in the Fermi gas model with equidistant spacing, because the same value $V_0 = 20$ MeV works for all neutron energies and two target nuclei among which one is doubly magic. This agreement is not restricted to the angular distributions, but extends to the energy spectra; an example is shown in Fig. 7.

We propose that the dependence $V_0(E_p)$ reflects the energy dependence of the effective neutron-proton interaction in nuclear matter, averaged over the relative energies contribution at $E_p = 25$ MeV and 80 MeV, respectively. It is well known that the strength of the $\Delta S = 0$, $\Delta T = 0$ component dominates the effective nucleon-nucleon interaction for

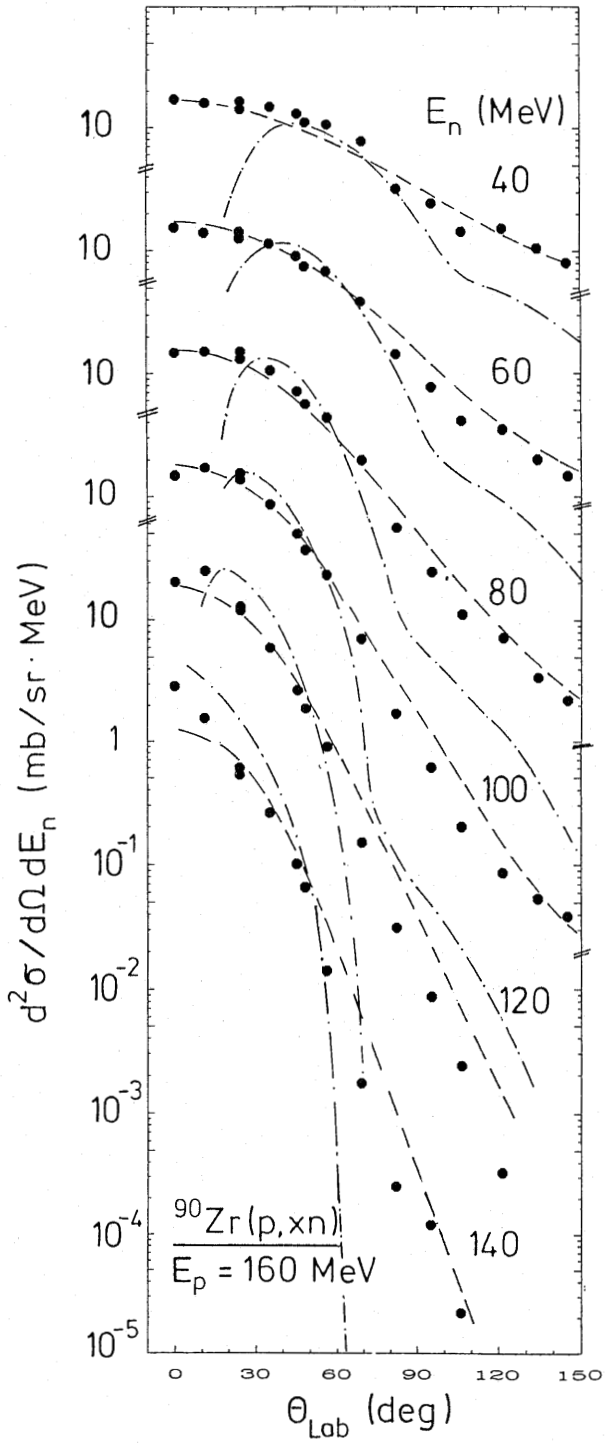

Figure 5. Angular distributions in comparison to the normalized results of Eq. (1) (dashed) and the GDH model prediction (dashed-dotted).

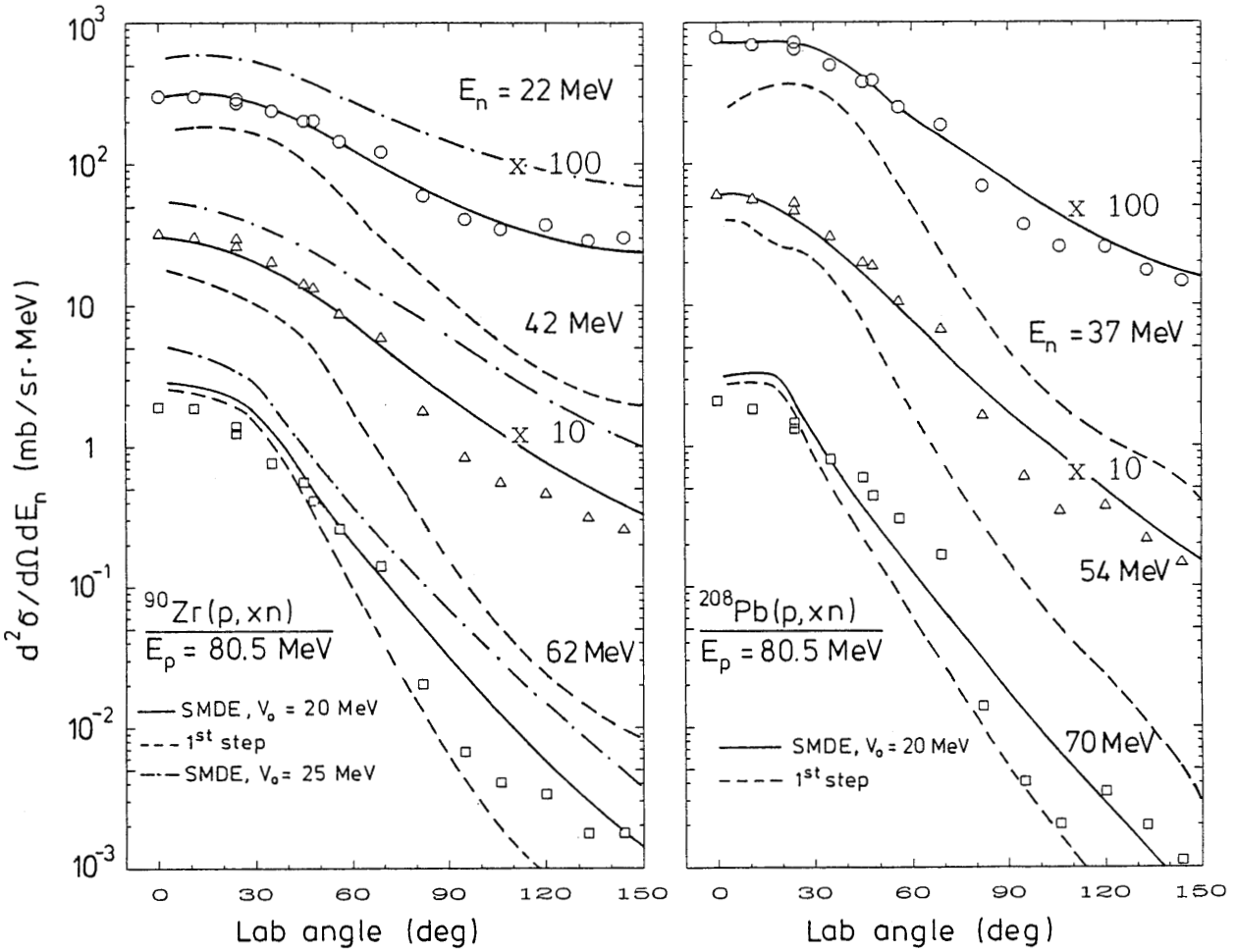

Figure 6. Comparison of experimental angular distributions and SMDE calculations with effective nucleon-nucleon interaction V_0.

the proton energies under discussion and decreases with increasing E_p. Evidence for such a dependence has also been found[21] in a DWBA analysis of $^{90}Zr(p,d_{0,1,2})^{89}Zr$ for E_p = 20–120 MeV; our reduction of V_0 by 25% is in almost quantitative agreement with that result. The conclusion, however, needs additional support that may come from the (p,n) calculations for E_p = 120 MeV and 160 MeV to be performed.

In summary, the (p,n) data presented provide evidence that the MSD mechanism is the dominant one for a broad range of ejectile energies in the continuum part, and that the higher step contributions are important even for the highest ejectile energies. The SMDE/SMCE model[7] give an adequate description of (p,n) data if it is assumed than the effective nucleon-nucleon interaction V_0 is not constant but decreases with increasing projectile energy.

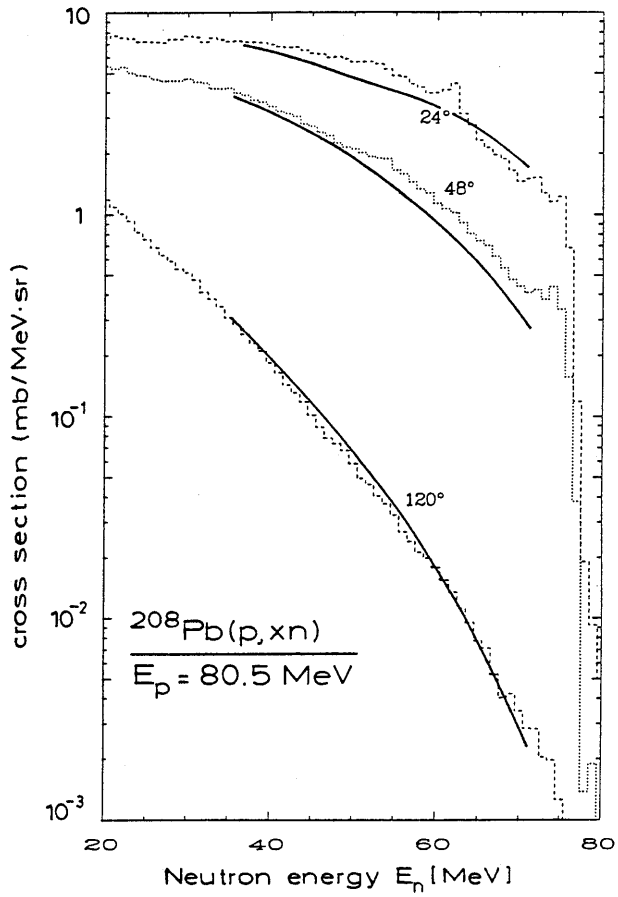

Figure 7. Experimental neutron energy spectra compared to SMDE calculations with $V_0 = 20$ MeV.

*Supported by the BMFT (Vorhaben 06 HH 175) and by the DOE under contract No. W-7405-Eng-48.

1. E. Mordhorst, et al., Phys. Rev. **C34**,103 (1986) and references therein.
2. J. Bisplinghoff, Phys. Rev. **C 33**, 1569 (1986).
3. M. Blann, et al., Phys. Rev. **C 30**, 1493 (1984).
4. H. Gruppelaar, et al., Riv. Nuov. Cim. **9**, 1 (1986).
5. K. Sato, Phys. Rev. **C32**, 647 (1985).
6. T. Tamura, et al., Phys. Rev. **C 26**, 379 (1982).
7. H. Feshbach, et al., Ann. Phys. (N.Y.) **125**, 429 (1980).
8. R. Bonetti, et al., Phys. Rev. **C 27**, 1003 (1983).
9. R. Bonetti, et al., Phys. Rev. **C 24**, 71 (1981).
10. R. Bonetti, et al., Phys. Rev. **C 28**, 980 (1983)
11. A.M. Kalend, et al., Phys. Rev. **C 28**, 105 (1983).
12. M. Blann, et al., Phys. Rev. **C 28**, 1475 (1983).
13. C. Kalbach, Report LA-UR-87-4139 (1987).
14. D.L. Friesel, Nucl. Instr. and Meth. **B10/11**, 864 (1985).
15. C.D. Goodman, et al., IEEE Trans. Nucl. **26**, 2248 (1979).
16. R.A. Cecil, et al., Nucl. Instr. and Meth. **161**, 439 (1979).

17. T. Taddeucci, et al., Phys. Rev. C **33**,746 (1986).
18. C. Kalbach, et al., Phys. Rev. C **23**, 122 (1981).
19. Y. Holler, et al., Nucl. Phys. **A442**, 79 (1985).
20. P. Schwandt, et al., Phys. Rev. C **26**, 55 (1982).
21. S. Kosugi, et al., Phys. Lett. **127B**, 389 (1983).

A STUDY OF THE (^{3}He,t) CHARGE-EXCHANGE REACTION AT E(^{3}He)=200 MeV

J. Janecke, F.D. Becchetti, V. Cianciolo, A. Nadasen, D. Roberts
University of Michigan, Ann Arbor, Michigan 48128

G.P.A. Berg, R. Sawafta, E.J. Stephenson
Indiana University Cyclotron Facility, Bloomington, Indiana 47405

M.N. Harakeh
Vrije Universiteit, Amsterdam, The Netherlands

S.Y. van der Werf
Kernfysisch Versneller Instituut, Groningen, The Netherlands

The (^{3}He,t) charge-exchange reaction has been studied at a bombarding energy of 200 MeV on 12 targets ranging from ^{12}C to ^{244}Pu including ^{90}Zr, ^{120}Sn, ^{208}Pb and five radioactive actinide targets. The objective of this work was to establish the feasibility of taking data at zero degrees with the K600 spectrometer and to determine the sensitivity of this charge-exchange reaction to spinflip and non-spinflip transitions. The results could then be compared to the (^{3}He,t) charge-exchange reaction at higher bombarding energies[1] and to (p,n) charge exchange[2]. The selectivity to non-spinflip L=0 transitions is of particular interest for the observation of isobaric analog states (IAS) and certain isovector giant resonances. In a particular application, properties of IAS were measured with emphasis on heavy nuclei.

The experiment was carried out with the K600 magnetic spectrometer at zero degrees. The ^{3}He^{++} beam entered the spectrograph and hit a beam stop inside the first dipole magnet. The beam stop was electrically insulated so that the beam current could be read directly from it. Background in the focal plane detector due to particles originating from the beam stop and from beam halo was low when proper precautions were taken. Singly-ionized ^{3}He$^+$ particles produced in the target with an intensity on the order of 10^{-8} compared to the incident beam reached the focal plane where they increased the event rate by approximately 30% unless eliminated with an absorber in front of the focal plane detector. Spectra were measured mostly in singles mode, but preliminary coincidence spectra were also obtained in a few instances. In this case, decay protons from unbound states were detected in the scattering chamber at backward angles with two large-area Li-drifted Si detectors.